Magnetic excitations in the *XY*-pyrochlore antiferromagnet $Er_2Ti_2O_7$

S. S. Sosin and L. A. Prozorova
P. L. Kapitza Institute for Physical Problems, RAS, 119334 Moscow, Russia

M. R. Lees, G. Balakrishnan, and O. A. Petrenko
Department of Physics, University of Warwick, Coventry CV4 7AL, United Kingdom
(Received 27 May 2010; published 15 September 2010)

The XY-pyrochlore antiferromagnet $Er_2Ti_2O_7$ is studied by heat-capacity measurements and electron-spin resonance spectroscopy performed on single-crystal samples. The magnetic phase diagrams are established for two directions of applied field, $H\|[100]$ and $H\|[111]$. In the magnetically ordered phase observed below $T_N = 1.2$ K, the magnetic excitation spectrum consists of a Goldstone mode acquiring an isotropic gap in an applied field, and another mode with a gap softening in the vicinity of a field-induced phase transition. This second-order transition takes place at a critical field H_c above which the magnetization process is accompanied by a canting of the magnetic moments off their local "easy planes." The specific-heat curves for $H\|[100]$ ($H \gg H_c$) are well described by a model presuming a single dispersionless excitation mode with the energy gap obtained from the spectroscopic measurements.

DOI: 10.1103/PhysRevB.82.094428 PACS number(s): 75.30.Sg, 75.50.Ee, 75.30.Kz

I. INTRODUCTION

Compounds with strong geometrical frustration of magnetic bonds have attracted much attention due to the unusual properties of their manifold ground states and their peculiar spin dynamics. For some systems, the degeneracy of the ground state in the nearest-neighbor (NN) exchange approximation is macroscopic, which leads to (i) delayed magnetic ordering and a wide temperature interval with a short-range correlated state, the so-called cooperative paramagnet,[1] and to (ii) an enhanced role for other interactions in the eventual formation of a long-range order state at low temperature. Different mechanisms for lifting the macroscopic degeneracy and selecting a specific ground state are a matter of individual consideration for each system. In the case of pyrochlore magnets, (nearly) fully ordered states, cooperative paramagnetic states, spin-glass, and spin-ice states have all been observed in different materials depending on the types of interactions in them.[2]

Experimental investigations of excitation spectra often provide the only viable method of determining a specific set of interactions to be taken into account for an individual magnetic compound. For example, in a Heisenberg pyrochlore magnet $Gd_2Sn_2O_7$, where the four-sublattice structure with $\mathbf{k}=0$ (a so-called plane cross or a Palmer-Chalker state) is found at low temperature,[3] the spin-wave calculations performed for this type of ordering with known microscopic parameters of exchange, dipolar interactions and a single-ion anisotropy[4,5] are in perfect agreement with the experimentally obtained picture, thus demonstrating the validity of this description.

Unlike the Gd-based Heisenberg pyrochlores, erbium titanate $Er_2Ti_2O_7$ has a strong local XY-type anisotropy of magnetic moments due to the large orbital momentum of Er^{3+} ions ($L=6$) which is not quenched by the crystal field (CF). The Curie-Weiss temperature in $Er_2Ti_2O_7$ obtained from the susceptibility data points to an antiferromagnetic NN exchange interaction. In this case, the XY anisotropy does not completely lift the degeneracy but reduces its degree down to $N^{2/3}$, where N is the number of magnetic ions in the system (see, e.g., Ref. 6). For a pyrochlore system with ferromagnetic NN exchange (as is the case for the ytterbium titanate, $Yb_2Ti_2O_7$), the classical ground state is expected to be nondegenerate. Nevertheless, $Yb_2Ti_2O_7$ remains disordered down to the low temperatures and has been recently shown to undergo an ordering transition only in an applied magnetic field.[7]

Depending on the temperature interval of susceptibility data fitting, the value of Θ_{CW} varies from −13 K in the higher temperature limit 80–300 K (Ref. 8) to −22 K if determined from data collected at temperatures below 50 K.[9] $Er_2Ti_2O_7$ is known to undergo a second-order transition to a long-range ordered state at about 1.2 K.[10–12] A spherical neutron polarimetry experiment indicates that the magnetic structure is formed from six domains, all of which are equally occupied.[13] In addition, recent high-resolution neutron-diffraction measurements detect the coexistence of short- and long-range order.[14] Low-lying excitation modes ungapped in zero field and near a critical field of about 15 kOe are also observed in this experiment. Muon-spin-relaxation measurements show nonvanishing spin dynamics as the temperature approaches zero,[15] in contrast to the expectations for a conventional magnet.

The noncoplanar structure appearing below T_N is presumed to be induced by fluctuations,[6,12] but this model predicts a strong first-order phase transition, while experimentally it is found to be continuous. A mean-field model which includes single-ion anisotropy and anisotropic exchange interactions is capable of producing the required long-range order,[16] however thermal or quantum fluctuations are expected to be important in this material. Polarized neutron-diffraction measurements[17] suggest that in addition to crystal-field parameters, an anisotropic molecular field tensor must be included in order to reproduce the experimental values of the local susceptibility tensor.

We present the results of an extensive electron-spin resonance (ESR) study of $Er_2Ti_2O_7$, which is used as a high-resolution probe of the $q=0$ energy structure for different

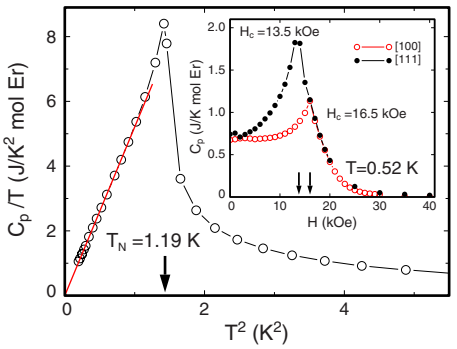

FIG. 1. (Color online) Specific heat divided by temperature of $Er_2Ti_2O_7$ in zero field. Solid line is $C_p/T \propto T^2$ fit for the low-temperature part of the curve. The inset shows the field dependencies of the specific heat at $T=0.52$ K: $H\|[100]$—○ and $H\|[111]$—●.

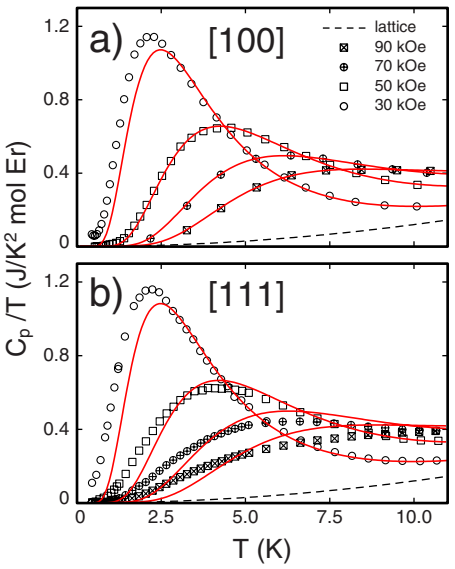

FIG. 2. (Color online) Temperature dependencies of the specific heat divided by temperature of $Er_2Ti_2O_7$ in various magnetic fields applied along the (a) [100] and (b) [111] directions. Solid lines represent the fits to Eq. (1) as described in the main text, the phonon contribution to the specific heat is shown by the dashed lines.

directions of an applied field. A Goldstone mode is observed and its linear increase with an applied magnetic field is traced. Additionally, we have detected a gapped mode softening in the vicinity of a critical field. The origin of both types of oscillation is discussed. Specific-heat measurements were also carried out for $H\|[100]$ and $H\|[111]$ to complement the previously reported results[14] for $H\|[110]$. The calorimetry results are compared with the ESR and inelastic neutron-scattering data[14] and an overall agreement between the different experimental methods is demonstrated.

II. EXPERIMENTAL PROCEDURES

A single-crystal sample of $Er_2Ti_2O_7$ was grown by the floating-zone technique.[18] Small thin plates of a characteristic size $1\times1\times0.2$ mm^3 (about 1 mg in mass) containing the (110) plane were cut out of the original larger sample. The plates were mounted in such a way that the magnetic field was applied in the sample plane in order to minimize the demagnetization effect. Specific heat was measured using a Quantum Design physical property measurement system calorimeter equipped with a ^{3}He option and a 90 kOe cryomagnet.

ESR measurements were carried out using a homemade transmission-type spectrometer built on a ^{3}He cryostat with a base temperature of 0.45 K. The lowest eigenfrequency of the resonant cavity was 25 GHz. The highest frequency was limited to about 70 GHz by the so-called "size effect," i.e., the condition that the half wavelength of the microwave radiation inside the sample is of the same order as the sample size. For the pyrochlore magnets, this limit is especially rigid because of their large magnetic permeability. It has been shown in case of another pyrochlore, $Gd_2Ti_2O_7$, that above this frequency limit a parasitic absorption (not directly related to magnetic excitation spectrum of the samples) can disguise its resonance pattern.[19]

III. EXPERIMENTAL RESULTS

The temperature dependence of the specific heat in zero external magnetic field is shown in Fig. 1. It demonstrates a sharp anomaly at $T_N=1.2$ K in close agreement with the previously obtained results. This peak corresponding to a second-order phase transition into a magnetically ordered state is followed by $C_p \propto T^3$ drop of specific heat on decreasing the temperature. The magnetic entropy of the system obtained by integrating the C_p/T curve with the phonon contribution subtracted (see below for details) saturates at the value of $R \ln 2$. This points to the effective $S=1/2$ pseudospin character of the magnetic Er^{3+} ions originating from the double degeneracy of its ground state in a crystal field.

In an applied magnetic field, the transition shifts to lower temperatures and becomes difficult to detect in the $C(T)$ curves. The transition is also traced by recording the field dependence of the specific heat at constant temperature. The $C(H)$ dependence measured for two different directions of the external magnetic field, $H\|[100]$ and [111], shows that the peak anomalies are easily detectable (see the inset of Fig. 1) and that their behaviors are quite anisotropic in nature with the transitions occurring at $H_c^{[100]}=16.5\pm0.5$ kOe and $H_c^{[111]}=13.5\pm0.5$ kOe.

The observed transformation of the $C(T)$ curves on increasing the external magnetic field up to and above the H_c for these two field directions is similar to the behavior reported in Ref. 14 for $H\|[110]$. In higher applied fields, the sharp low-temperature anomaly seen in the $C(T)$ curves is replaced by a much broader feature developing in the higher-temperature part of the curves (see Fig. 2).

Following the results of an inelastic neutron-scattering experiment for $H\|[110]$ in Ref. 14 which showed for the lower excitation mode the dispersion vanishing at $H \gg H_c$, one can attempt to approximate $Er_2Ti_2O_7$ in high fields as an ensemble of noninteracting two-level systems. In this case, the molar specific heat can be expressed in the form

$$C_p = \alpha R\left(\frac{\Delta}{kT}\right)^2 \frac{e^{-\Delta/kT}}{(1+e^{-\Delta/kT})^2} + \beta T^3, \qquad (1)$$

where the first term represents the Schottky anomaly (Δ is the gap value, $\alpha \simeq 1$ is a numerical coefficient), and the second term is the phonon contribution. Taking α, β, and Δ as fitting parameters, one can perfectly well reproduce the specific-heat curves in higher fields (50, 70, and 90 kOe) in Fig. 2(a) for $H\|[100]$ over the entire temperature range shown. For all scans we obtain $\alpha = 0.84 \pm 0.01$ and $\beta \simeq (1.33 \pm 0.03) \times 10^{-3}$ J/(K^4 mol Er). The latter value agrees well with the specific heat of an isomorphous nonmagnetic compound $Y_2Ti_2O_7$ (see, e.g., Ref. 20) rescaled to $Er_2Ti_2O_7$ by molar mass in the approximation that the Debye temperature $\theta \propto 1/\sqrt{M}$. The field dependence of the gap values is presented in the resulting phase diagram (Fig. 6) and discussed below. Only the high-temperature part of the heat capacity measured at $H = 30$ kOe can be satisfactorily described by Eq. (1), as the low-energy contributions to the entropy are not taken into account in this simple model. The observed behavior of the specific heat indicates that the high-field excitation spectrum may indeed be modeled as a set of two-level systems with a field-dependent gap while nearer to the critical field, a more important role is played by the dispersion of the excitation mode.

The specific heat reported by Ruff *et al.*[14] for a magnetic field along the [110] direction exhibits the same properties. The high-field $C_p(T)$ curves shown in Fig. 1 of Ref. 14 can also be described in the manner outlined above. The corresponding gap value at $H = 70$ kOe is shown on Fig. 6 for reference.

Using the same model, however, we could not obtain satisfactory fits to our data obtained for $H\|[111]$. The solid lines on the lower panel of Fig. 2 drawn with the same set of parameters as for $H\|[100]$ illustrate the point that some of the magnetic entropy for this field direction is redistributed to lower temperatures. One could suggest that the energy of the long-wave excitations grows more slowly for a magnetic field applied along the [111] axis than for other field directions. The relationship between the heat-capacity data and the results of the magnetic resonance measurements is discussed below.

The resonance absorption spectra recorded at the lowest experimentally available temperature of 0.45 K at constant frequency on increasing/decreasing field sweeps are presented in Fig. 3. Rather similar results have been obtained at $H < H_c$ for fields along the [100], [110], and [111] axes. Two spectral lines of Lorentzian shape are observed below T_N. The resonance field of line 1 grows linearly with the increasing frequency while the position of line 2 shifts to lower fields. Their relative intensities vary with field direction but the half width of both lines lie in the interval $\Delta H_{1,2} \simeq 1-1.2$ kOe. The nearly frequency-independent resonance field of the second line in the vicinity of the critical field points to the possible complete softening of this resonance mode, although our experimental frequency limit does not allow for spectral records below 25 GHz (corresponding to energies of about 0.1 meV). At higher fields, for $H > H_c$, a third narrow line ($\Delta H_3 \simeq 0.2$ kOe) appears in the spectra for

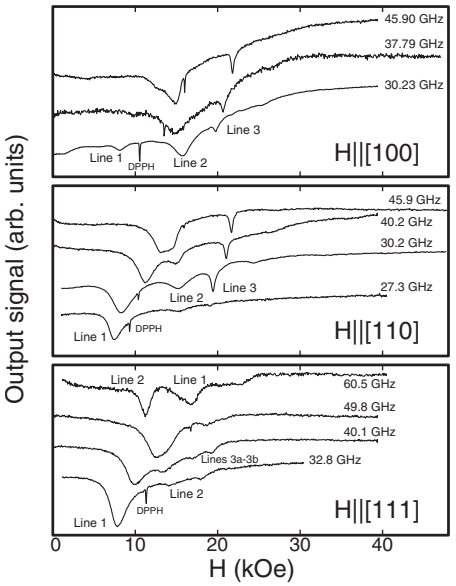

FIG. 3. Magnetic resonance absorption spectra in $Er_2Ti_2O_7$ recorded at the lowest experimental temperature of 0.45 K at different frequencies of the microwave radiation for the three principal orientations of the external magnetic field $H\|[100]$, [110], and [111]. Narrow weak peaks are the DPPH labels (a paramagnet with the g factor of 2.

$H\|[100]$ and [110] axes while for $H\|[111]$ axis an absorption of this type is not seen. Instead, two much broader spectral lines with considerably smaller intensities [lines 3a and 3b on the lowest panel of Fig. 3] are observed. A quantitative analysis of the frequency-field diagram is performed below.

A typical transformation of the resonance spectrum on increasing the sample temperature above the Néel point is shown in Fig. 4. The records at $\nu = 40.2$ GHz reveal an intensity loss for all three spectral lines on heating. Lines 1 and 2 almost disappear at the transition temperature (about 1.0 K and 0.8 K for the corresponding resonance fields). Although line 3 exists in the higher fields and is therefore not directly related to any low-field antiferromagnetic order, it is ob-

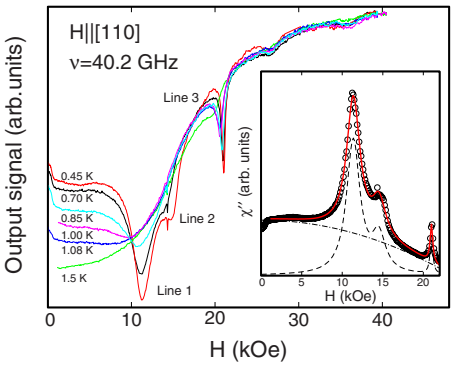

FIG. 4. (Color online) The temperature evolution of the absorption spectra of $Er_2Ti_2O_7$ measured at the frequency $\nu = 40.2$ GHz for a field parallel to [110]. The inset shows the field dependence of χ'' extracted from the absorption records, fitted by a sum of three Lorentzian spectral components (dashed line) on the nonresonant background (dashed-dotted line).

served only at low temperature, broadening and disappearing on warming above 1.5 K. As seen in Fig. 4, the absorption in the sample is accompanied by a broad nonresonant background gradually vanishing in the high-field limit. This background signal grows in amplitude on approaching the Nèel temperature and finally replaces the three lines of the low-temperature spectrum. Comparing the spectra recorded at various frequencies one finds that the background is excited only by the microwave field component directed along the external magnetic field. Therefore, the absorption is associated with the longitudinal oscillation of the magnetic moment and should be damped in the vicinity of the field at which the magnetization reaches its maximum value. A similar effect was observed in the Heisenberg pyrochlore system $Gd_2Ti_2O_7$ where the longitudinal susceptibility was supposed to result from a partial disorder of the magnetic ground state.[5] As in the present case, this mode had very strong relaxation (of unknown origin) which makes it impossible to observe other than in the form of a broad nonresonant background vanishing above the saturation field. Approximating the system as a set of "rigid" sublattices canted to the magnetic field, one obtains the slow response of the system to the microwave field to be $\chi \sim \cos^2 \varphi$, where φ is an angle between the sublattice and the field. Since the total magnetization of the system is $M=M_c \sin \varphi$ (M_c is a maximum magnetization), the resulting contribution of such a degree of freedom to the dynamic susceptibility of the sample can be estimated as $\chi'' \propto 1-(M/M_c)^2=1-(H/H_c)^2$ (H_c is a critical field). The above approach is qualitatively illustrated in the inset of Fig. 4. The imaginary part of the dynamic susceptibility extracted from the absorption spectrum record was fitted by a sum of three resonance lines of Lorentzian shape and a nonresonant background with H_c taken as a fitting parameter. The fit shown by the solid line was achieved for $H_c=23.6$ kOe which compares reasonably well to the value of the critical field. The same description works well in low fields for all the absorption data in which the amplitude of the background signal is comparable to the main resonance peak intensity. Less than perfect fit to the experimental data in higher fields (including the absence of a sharp kink in the vicinity of H_c) is not surprising for such a simple model as described above. Moreover, as discussed below, H_c is not a usual saturation field—the magnetization does not reach a maximum at $H=H_c$ and continues to grow with increasing field above H_c albeit with a lower rate.

IV. DISCUSSION

For comparison with the experimentally observed spectra, one should first determine the g values of a single Er^{3+} ion in a CF for the various directions of an external magnetic field. The total momentum in the ground state of Er^{3+} ion (electron shell configuration $4f^{11}6s^0$) is $J=15/2$ ($L=6$, $S=3/2$). The CF of a trigonal D_{3d} point symmetry at the erbium sites (the threefold axes are parallel to local [111] axes) splits the 16-fold state into eight doublets. A calculation of this splitting using the CF Hamiltonian parameters rescaled from another pyrochlore compound $Ho_2Ti_2O_7$ (given in Ref. 21) describes well the observed gaps between the lowest and two excited CF levels[12] and gives the following expression for the lowest Kramers doublet: $\psi_{1,2}=0.543|\mp\frac{11}{2}\rangle \pm 0.238|\mp\frac{5}{2}\rangle -0.563|\pm\frac{1}{2}\rangle \mp 0.388|\pm\frac{7}{2}\rangle +0.426|\pm\frac{13}{2}\rangle$. Using these wave functions, one can easily calculate the single-ion energy splitting under magnetic field applied at an arbitrary angle α with respect to a local trigonal axis,

$$\Delta\varepsilon = \mu_B H \sqrt{g_\parallel^2 \cos^2 \alpha + g_\perp^2 \sin^2 \alpha}, \tag{2}$$

where $g_\parallel=0.24$ and $g_\perp=7.6$ are the g factors parallel and perpendicular to [111]. A more general calculation which involves the solution of a total atomic Hamiltonian and uses high-temperature susceptibility data in the fitting procedure gives slightly different lowest doublet wave functions but the same g values.[8] It should be noted that recent neutron-scattering measurements[17] have determined a much less pronounced XY anisotropy of the local susceptibility tensor with the values of $g_\parallel=2.6$ and $g_\perp=6.8$. When the field is applied along [100] axis, all four magnetic moments in the unit cell are in equivalent positions with $\cos \alpha=1/\sqrt{3}$. Field directions $H\|[110]$ and [111] create two nonequivalent positions with $\cos \alpha_1=\sqrt{2/3}$, $\cos \alpha_2=0$ and $\cos \alpha_1=1$, $\cos \alpha_2=2\sqrt{2}/3$, respectively. The corresponding effective $\tilde{g}$ values are collected in Table I.

TABLE I. The calculated effective $\tilde{g}$ values of a lowest Kramers doublet splitting in a magnetic field and the slope of magnetic resonance branch 3 observed above H_c for three principal field directions.

	Refs. 8 and 12	Ref. 17	$\nu_3(H)$
[100]	6.2	5.8	5.4
[110]	4.4, 7.6	4.5, 6.8	5.4
[111]	0.2, 7.1	2.6, 6.5	4.6

Let us now analyze the resonance spectra measured at the temperature 0.45 K for the three different orientations of the external magnetic field. The frequency-field diagram is presented in Fig. 5. The resonance spectrum observed below the critical field H_c consists of two branches. Branch 1 is increasing in field and can be approximated by a linear dependence $\nu=\gamma H$ with the value of γ slightly dependent on the field direction: $\gamma_{[100]}=3.8\pm0.1$ GHz/kOe, $\gamma_{[110]}=3.6\pm0.1$ GHz/kOe, and $\gamma_{[111]}=4.1\pm0.1$ GHz/kOe, which correspond to effective g values 2.7, 2.6, and 2.9, respectively. This linear in field gap signifying the existence of a Goldstone mode at zero magnetic field is quite unexpected for a strongly anisotropic magnetic system where all the acoustic modes should be influenced by spin-orbit coupling. The residual gap due to a possible (within the experimental accuracy) deviation from the linear extrapolation to zero field does not exceed a value ~ 10 GHz $\simeq 0.04$ meV. One should also note that the power-law dependence of the specific heat $C_p \propto T^3$ extending to very low temperatures[10,11] confirms the existence of gapless magnetic excitations at zero field. Obviously, this mode cannot be interpreted in terms of a single-ion splitting. The observed increase in the gap, which is linear in field, should be ascribed to a uniform oscillation of the magnetization resulting from the in-phase

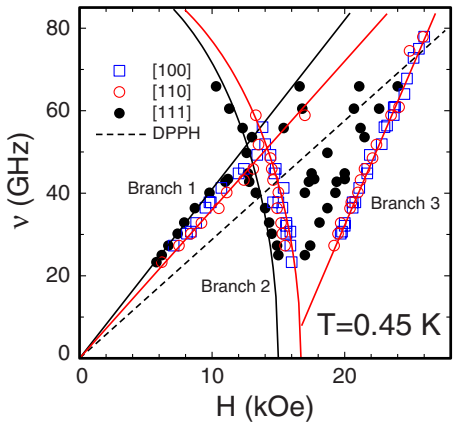

FIG. 5. (Color online) The frequency-field diagram obtained from the resonance spectra of $Er_2Ti_2O_7$ at $T=0.45$ K (shown in Fig. 3): □—$H\|[100]$, ○—$H\|[110]$, and ●—$H\|[111]$. Fits to all observed spectral modes are shown by solid lines, dashed line is a DPPH label corresponding to the paramagnet with $g=2$.

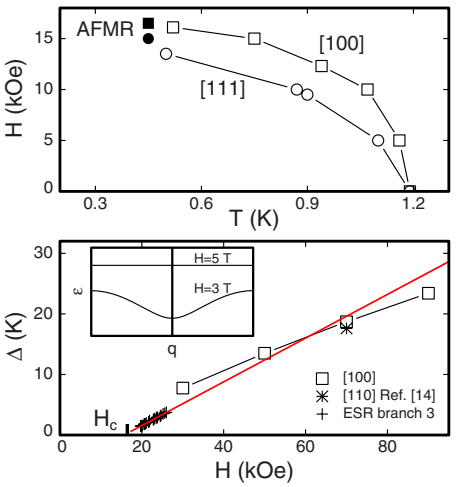

FIG. 6. (Color online) Upper panel: the phase diagram of $Er_2Ti_2O_7$ for $H\|[100]$ (□,■) and $H\|[111]$ (○, ●) obtained from specific heat and magnetic resonance data respectively. Lower panel: gap values determined from fitting the $C_p(T)$ curves for $H\|[100]$ by Eq. (1); $\nu(H)$ dependence of ESR branch 3 is shown by crosses, solid line is a linear extrapolation of this branch to high fields. The schematic transformation of the excitation spectrum at high fields (based on experimental data from Ref. 14) is given in the inset.

spin motion in the planes perpendicular to the local [111] axes.

Branch 2 has a gap that diminishes quickly in the vicinity of the critical field. Although the high-frequency measurements were hindered by the size effect and the zero-field gap of branch 2 is not determined from our experiment, one can relate this branch to the gapped mode with $\Delta_0 \simeq 0.4$ meV observed by inelastic neutron scattering.[14] The field dependence of this branch in the vicinity of the second-order transition $H=H_c$ is similar to the behavior of the optical branch near the spin-flip transition: $\Delta \sim \Delta_0\sqrt{1-(H/H_c)^2}$. Using this formula one can satisfactorily approximate the field dependence of branch 2 for all three field orientations and therefore estimate the critical field values: $H_c^{[100]}=16.5\pm0.5$ kOe; $H_c^{[110]}=16.0\pm0.5$ kOe, and $H_c^{[111]}=15.0\pm0.5$ kOe. An optical branch with an analogous field dependence was observed in the spectrum of the Heisenberg pyrochlores $Gd_2Ti_2O_7$ and $Gd_2Sn_2O_7$. It corresponds to the out-of-phase oscillations of spins in local "easy" planes.

The analysis of the relative intensities of the magnetic Bragg peaks[14] shows that the field-induced transformation of the magnetic structure can roughly be described as a rotation of magnetic moments in their local easy planes. The critical field is determined by the maximum value of the magnetic moment which can be achieved without canting from these planes. This geometric restriction was analyzed theoretically and the corresponding critical fields were calculated.[22] The ratio $H_c^{[100]}/H_c^{[110]}=2\sqrt{2}/(\sqrt{3}+1)\simeq 1.04$ is in agreement with our results within the experimental accuracy while the theoretical value for $H_c^{[100]}/H_c^{[111]}=7\sqrt{2}/(3\sqrt{3}+\sqrt{6})\simeq 1.3$ appears to be considerably larger than the value 1.1 obtained from our ESR experiments. In contrast, the corresponding ratio of critical fields measured by specific heat, $16.5:13.5\simeq 1.2$ demonstrates better agreement with the model. The resulting phase diagram obtained on the basis of both measurements with $H\|[100]$ and [111] are shown in the upper panel of Fig. 6.

At $H>H_c$, for two directions of the magnetic field $H\|[100]$ and [110], there exists a single gapped resonance mode that increases linearly in field as $\nu_3=\Delta(H_c)+\tilde{\gamma}(H-H_c)$, with roughly the same effective gyromagnetic ratio $\tilde{\gamma}=7.5$ GHz/kOe ($\tilde{g}=5.4$) and $\Delta(H_c)\leq 5$ GHz. For $H\|[111]$, a resonance mode of this type is absent and is replaced by two spectral components with smaller amplitudes and much larger linewidths giving evidence for increased damping of these oscillations. Their energies also grow linearly in field with somewhat smaller $\tilde{\gamma}=6.4$ GHz/kOe ($\tilde{g}=4.6$).

Obviously, the influence of a magnetic field on the collective excitations above H_c is more associated with the single-ion level splitting than in the antiferromagnetic phase. The linear in field increase in the gap observed for $H\|[100]$ is rather close to the single-ion $\tilde{g}$ factor (especially to the one reported in Ref. 17) while for [110] the $\tilde{g}$ factor lies between the values for two nonequivalent positions (see Table I). The absence of a well-defined collective oscillation mode in the third field direction $H\|[111]$ is most likely the result of a large difference of single-ion $\tilde{g}$ values in two nonequivalent positions which should destroy the coherent precession of an ensemble of spins with an average frequency.

One can also establish a relationship between the increase in the gap as observed directly by the ESR spectroscopy and the evolution of the specific-heat curves under field. The gap values obtained from the specific heat in the approximation of a single dispersionless gapped mode (two-level Schottky anomalies) and the field dependence of branch 3 at $H\|[100]$ are presented in the lower panel of Fig. 6. The difference between them at fields just above the transition results from the effect of dispersion on the specific heat which is not taken into account in our fitting. The convergence of the Schottky anomaly gaps to the high-field linear extrapolation of branch 3 is evidence of a decrease in the dispersion of this

mode in the high-field limit. A similar effect, shown schematically in the inset of Fig. 6, was directly observed in inelastic neutron-scattering experiments for $H\|[110]$. The agreement between ESR and specific-heat data (single ESR branch and satisfactory modeling by a two-level system) is also established for $H\|[110]$. In contrast, the failure of such a model for $H\|[111]$ (see Fig. 2) can be considered as a bulk analog of the absence of a well defined excitation branch in the ESR measurements.

V. SUMMARY

In conclusion, the specific heat and the low-temperature magnetic resonance spectra were studied in the XY-pyrochlore antiferromagnet $Er_2Ti_2O_7$. A Goldstone mode with a gap linearly dependent on the applied field is observed in the ordered state. Another mode has a zero-field gap consistent with the inelastic neutron-scattering results which softens in the vicinity of the second-order transition driven by magnetic field. Presumably, these collective modes correspond to in-phase and out-of-phase oscillations of spins in local easy planes. The critical field values are determined in three principal field orientations both from ESR and specific-heat measurements. This transition is associated with the maximum possible spin reorientation without canting from their planes. In the high-field phase the excitation spectrum for two field directions $H\|[100]$ and $H\|[110]$ consists of a single branch. The linear increase in the gap of this branch in magnetic field is somewhat related to the g-factor values characteristic of a splitting of a single-ion lowest doublet. The specific-heat curves observed at high fields demonstrate a Schottky-type anomaly with a gap that also increases with field. No well-defined excitation mode was observed above H_c at $H\|[111]$. Accordingly, the specific heat in strong magnetic fields does not demonstrate a two-level splitting with a single gap. A large difference in g factors for the two nonequivalent positions of the magnetic ions with respect to the field is suggested to account for the absence of a collective excitation mode. Our measurements provide a framework with which to calculate the excitation spectrum in $Er_2Ti_2O_7$ using an effective pseudospin-1/2 model.

ACKNOWLEDGMENTS

The authors thank M. E. Zhitomirsky for fruitful discussions. The work at Kapitza Institute is supported by the RFBR under Grant No. 10-02-01105. The work at Warwick is supported by the EPSRC under Grant No. EP/E011802. S.S.S is also grateful to LIA LPTMS for the financial support of the research visit to CEA Grenoble.

[1] J. Villain, Z. Phys. B **33**, 31 (1979).
[2] J. S. Gardner, M. J. P. Gingras, and J. E. Greedan, Rev. Mod. Phys. **82**, 53 (2010).
[3] A. S. Wills, M. E. Zhitomirsky, B. Canals, J.-P. Sanchez, P. Bonville, P. Dalmas de Réotier, and A. Yaouanc, J. Phys.: Condens. Matter **18**, L37 (2006).
[4] J. A. Quilliam, K. A. Ross, A. G. Del Maestro, M. J. P. Gingras, L. R. Corruccini, and J. B. Kycia, Phys. Rev. Lett. **99**, 097201 (2007).
[5] S. S. Sosin, L. A. Prozorova, P. Bonville, and M. E. Zhitomirsky, Phys. Rev. B **79**, 014419 (2009).
[6] J. D. M. Champion and P. C. W. Holdsworth, J. Phys.: Condens. Matter **16**, S665 (2004).
[7] K. A. Ross, J. P. C. Ruff, C. P. Adams, J. S. Gardner, H. A. Dabkowska, Y. Qiu, J. R. D. Copley, and B. D. Gaulin, Phys. Rev. Lett. **103**, 227202 (2009).
[8] P. Dasgupta, Y. Jana, and D. Ghosh, Solid State Commun. **139**, 424 (2006).
[9] S. T. Bramwell, M. N. Field, M. J. Harris, and I. P. Parkin, J. Phys.: Condens. Matter **12**, 483 (2000).
[10] H. W. J. Blöte, R. F. Wielinga, and W. J. Huiskamp, Physica (Amsterdam) **43**, 549 (1969).
[11] R. Siddharthan, B. S. Shastry, A. P. Ramirez, A. Hayashi, R. J. Cava, and S. Rosenkranz, Phys. Rev. Lett. **83**, 1854 (1999).
[12] J. D. M. Champion, M. J. Harris, P. C. W. Holdsworth, A. S. Wills, G. Balakrishnan, S. T. Bramwell, E. Cizmar, T. Fennell, J. S. Gardner, J. Lago, D. F. McMorrow, M. Orendac, A. Orendacova, D. McK. Paul, R. I. Smith, M. T. F. Telling, and A. Wildes, Phys. Rev. B **68**, 020401(R) (2003).
[13] A. Poole, A. S. Wills, and E. Lelievre-Berna, J. Phys.: Condens. Matter **19**, 452201 (2007).
[14] J. P. C. Ruff, J. P. Clancy, A. Bourque, M. A. White, M. Ramazanoglu, J. S. Gardner, Y. Qiu, J. R. D. Copley, M. B. Johnson, H. A. Dabkowska, and B. D. Gaulin, Phys. Rev. Lett. **101**, 147205 (2008).
[15] J. Lago, T. Lancaster, S. J. Blundell, S. T. Bramwell, F. L. Pratt, M. Shirai, and C. Baines, J. Phys.: Condens. Matter **17**, 979 (2005).
[16] P. A. McClarty, S. H. Curnoe, and M. J. P. Gingras, J. Phys.: Conf. Ser. **145**, 012032 (2009).
[17] H. Cao, A. Gukasov, I. Mirebeau, P. Bonville, C. Decorse, and G. Dhalenne, Phys. Rev. Lett. **103**, 056402 (2009).
[18] G. Balakrishnan, O. A. Petrenko, M. R. Lees, and D. McK. Paul, J. Phys.: Condens. Matter **10**, L723 (1998).
[19] S. S. Sosin, L. A. Prozorova, A. I. Smirnov, P. Bonville, G. Jasmin-Le Bras, and O. A. Petrenko, Phys. Rev. B **77**, 104424 (2008).
[20] N. P. Raju, M. Dion, M. J. P. Gingras, T. E. Mason, and J. E. Greedan, Phys. Rev. B **59**, 14489 (1999).
[21] S. Rosenkranz, A. P. Ramirez, A. Hayashi, R. J. Cava, R. Siddharthan, and B. S. Shastry, J. Appl. Phys. **87**, 5914 (2000).
[22] V. N. Glazkov, M. E. Zhitomirsky, A. I. Smirnov, H.-A. Krug von Nidda, A. Loidl, C. Marin, and J.-P. Sanchez, Phys. Rev. B **72**, 020409(R) (2005).